

## Experimental Observation of Picosecond Pulse Narrowing and Solitons in Optical Fibers

L. F. Mollenauer, R. H. Stolen, and J. P. Gordon

*Bell Telephone Laboratories, Inc., Holmdel, New Jersey 07733*

(Received 17 July 1980)

This paper reports narrowing and splitting of 7-ps-duration pulses from a mode-locked color-center laser by a 700-m-long, single-mode silica-glass fiber, at a wavelength (1.55  $\mu\text{m}$ ) of loss and large but negative group-velocity dispersion. At certain critical power levels, the observed behavior is characteristic of solitons.

PACS numbers: 42.65-k

A number of years ago, Hasegawa and Tappert<sup>1</sup> pointed out that nonlinearity of the index of refraction ( $n - n_0 = \frac{1}{2} n_2 |E|^2$ ) could be used to compensate the pulse broadening effect of dispersion in low-loss optical fibers. Although their work focused on the simplest stable pulse, computer<sup>2</sup> and analytic<sup>3-5</sup> studies have revealed the existence of a number (unlimited in principle) of such self-maintaining pulses, or (envelope) solitons. Solitons of higher order than the fundamental are self-maintaining in the sense that their pulse shapes are *periodic* with propagation.

In this Letter we report the first experimental observation in optical fibers of pulse compression and pulse splitting, and we show this behavior, at certain critical power levels, to be characteristic of higher-order solitons. Although solitons are known and studied experimentally in other branches of physics, such studies are often fraught with difficulty,<sup>6</sup> in particular because of transverse instabilities. By contrast, single-mode optical fibers offer a stable, simple, and well-characterized medium for such studies. Of equal importance, our experiments suggest a number of applications; nearly lossless compression of picosecond pulses is but one of these.

Two recent developments have made the soliton experiments feasible: (1) The realization<sup>7,8</sup> of single-mode silica-glass fibers having low loss (as low as 0.2 dB/km)<sup>7</sup> in the region ( $\lambda \gtrsim 1.3 \mu\text{m}$ ) of negative group-velocity dispersion and (2) mode-locked color-center lasers<sup>9</sup> capable of tuning over that same region. The requirement for negative group-velocity dispersion<sup>10</sup> can be understood as follows: Phase self-modulation<sup>11,12</sup> (due to the nonlinearity) tends to lower frequencies in the leading half of the pulse and to raise those in the trailing half. Negative dispersion is required for such a "chirp" to produce subsequent pulse compression. Furthermore, the larger the magnitude of dispersion, the more quickly the compression and other effects develop. Therefore, to minimize the required fiber length,

and to approximate most closely the ideal of a lossless medium, we have chosen to work in the loss minimum at 1.55  $\mu\text{m}$ .

The source was a synchronously pumped, mode-locked laser utilizing  $F_2^+$  centers in NaCl. Except for a different tuning range (1.35–1.75  $\mu\text{m}$ ), it was similar in construction (including the same pump source) and performance to the KF,  $F_2^+$ -center laser described earlier<sup>9</sup> and used for pulse propagation studies<sup>13</sup> at 1.3  $\mu\text{m}$ . However, the soliton experiments required two important modifications: (1) The ratio of cavity lengths was made 1:1, in order to have only one output pulse per pump input pulse; thus a certain essential uniformity of amplitude from pulse to pulse was guaranteed. (2) A birefringent tuning element (sapphire, 4 mm thick) was added to the cavity. This forced the laser to produce pulses of product  $\Delta t \Delta f \cong 0.18$ , where  $\Delta t$  and  $\Delta f$  refer to full widths at half maxima of the corresponding distributions. Note that this product lies between the minimum for  $\text{sech}^2$  pulses (0.315) and that for a decaying exponential (0.11). Such tight frequency definition is required to allow observation of well-resolved soliton effects.

The rest of the apparatus is shown schematically in Fig. 1. Its function is to allow for measurement (by autocorrelation) of both laser and fiber output pulse shapes. Simultaneous measurement of the two pulse shapes is achieved in only one autocorrelator through use of a simple time-sharing scheme. For further details, see the caption to Fig. 1.

Figure 2 shows the experimentally determined fiber output (pulse shapes and frequency spectra) at certain critical power levels. Power in the fiber core was varied by adjustment (focusing of  $L_1$ ) of the input coupling. The reported peak powers were obtained by multiplying the time average values, measured at the output end, by a duty factor ( $\cong 1200$ ) appropriate to the measured laser pulse width for each run and the 100-MHz pulse repetition rate.

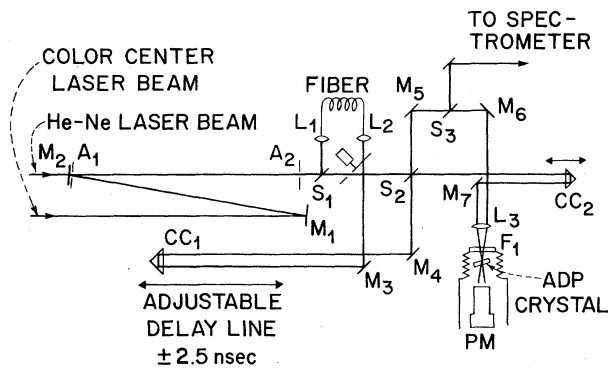


FIG. 1. Schematic of the apparatus.  $M_1$ ,  $M_2$ ,  $A_1$ , and  $A_2$  constitute a simple beam-aiming device. At  $S_1$ , the beam is split between "fiber" and "laser" channels. The chopper alternately blocks the two beams before they enter the autocorrelator ( $S_2$ ,  $M_5$ ,  $M_6$ ,  $M_7$ ,  $CC_2$ , etc.); the resultant photomultiplier signals (from noncollinear second harmonic generation in the ammonium dihydrogen phosphate crystal) are then separated out electronically.  $F_1$ , a slab of Si, passes 1.55- $\mu\text{m}$  light and rejects room light. (The adjustable delay line is needed only for cross-correlation measurements, not reported on here.)

At fiber powers considerably lower than the minimum reported there was no significant increase in pulse width. Therefore, the broadening seen at the  $P = 0.3 \text{ W}$  level is essentially that

due to dispersion alone; furthermore, it agrees with that calculated<sup>14</sup> from the known fiber dispersion at  $\lambda = 1.55 \mu\text{m}$  [ $D \cong -16(\text{ps}/\text{nm})/\text{km}$ ]. However, from then on, as the power was raised, we observed a continuous change in pulse shape, as follows: At first, the pulses steadily narrowed until, at  $P = 1.2 \text{ W}$ , they reduced to the input width; they then narrowed further to a minimum (2 ps) at  $P = 5 \text{ W}$ ; at still higher powers, the broad base began to rise and split. The curve shown for 11.4 W represents the first well resolved splitting; note that the threefold splitting in autocorrelation corresponds to a twofold splitting of the pulse itself. Similarly, the fivefold splitting (only partly resolved) seen at  $P = 22.5 \text{ W}$  corresponds to a threefold splitting of the real pulse. To see how this behavior is characteristic of solitons at the cited power levels, we must examine the known solitary solutions to the wave equation.

It can be shown<sup>15</sup> that the pulse envelope function,  $u(z, t)$ , satisfies the nonlinear equation

$$i \left( \frac{\partial u}{\partial z} + k_1 \frac{\partial u}{\partial t} \right) = -\frac{k_2}{2} \frac{\partial^2 u}{\partial t^2} + \kappa |u|^2 u, \quad (1)$$

where  $k_1 = \partial k / \partial \omega$ ,  $k_2 = \partial^2 k / \partial \omega^2$ , and  $\kappa = \frac{1}{2} k_0 n_2 / n_0$ . Equation (1) is reduced to the dimensionless non-

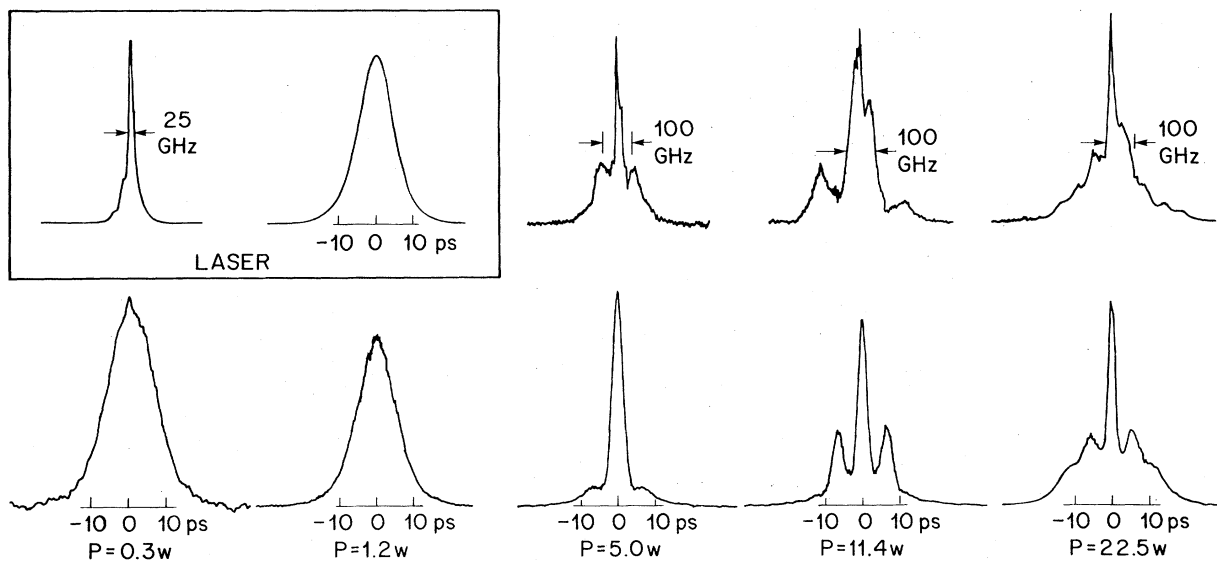


FIG. 2. Below: Autocorrelation traces of the fiber output as a function of power. Above: Corresponding frequency spectra. Inset: Similar data for the direct laser output. There is no absolute intensity scale here; the various curves have been roughly normalized to a common height. Corresponding to the fiber data, from low to high power, the laser pulse widths were 7.2, 7.0, 6.1, 6.8, and 6.2 ps, respectively. See text.

linear Schrödinger equation

$$i\partial v/\partial \xi = \frac{1}{2}\partial^2 v/\partial s^2 + |v|^2 v \quad (2)$$

by the transformation

$$s = \tau^{-1}[t - k_1 z], \quad (3a)$$

$$\xi = |k_2| \tau^{-2} z, \quad (3b)$$

$$v = \tau(\kappa/|k_2|)^{1/2} u. \quad (3c)$$

Note that the arbitrary time scale  $\tau$  in this transformation allows a pulse of standard duration in the dimensionless retarded-time variable  $s$  to correspond to a pulse of any desired duration in time  $t$ .

Equation (2) with the initial condition  $v(0, s) = a \operatorname{sech}(s)$  was studied analytically in Ref. 5. The solitary solutions obtain whenever  $a$  is an integer  $N$ . For  $N=1$ , the pulse remains forever like that at the input, but for higher  $N$ , the solutions have period  $\xi = \pi/2$ . Highlights of one period of the  $N=2$  and  $N=3$  solitons are shown in Fig. 3. It should also be noted that the  $N=4$  soliton (not shown for lack of space) exhibits a three-fold splitting at  $\xi = \pi/4$ , with the central peak large relative to its satellites.<sup>16</sup>

When transformed to ordinary dimension, the soliton period becomes  $z_0 = \pi\tau^2/2|k_2|$ . From  $k_2 = D\lambda_{\text{vac}}^2/2\pi c$ , for the value of  $D$  cited earlier, and for  $\tau=4$  ps (corresponding to 7 ps full width at

half maximum), we obtain  $z_0 = 1260$  m. Thus, the pulse shapes seen at the output end of the 700 m ( $\cong \frac{1}{2} \times 1260$  m) fiber should be fairly close, at the appropriate power levels, to those of the  $\xi = \pi/4$  curves of Fig. 3.

By now it should be clear that the behavior displayed in Fig. 2 for the higher levels corresponds to the  $N=1, 2, 3$ , and 4 solitons, respectively. Note that the quantity  $P/N^2 = P_0$  is nearly constant, as required for relative integral amplitudes. A perfect fit is prevented by deviation of the fiber length from an exact half period, and by variation in the input pulse width.

The theory also predicts an absolute value for  $P_0$ . From Eq. (3c), the corresponding critical intensity is  $I_0 = n_0 c \lambda_{\text{vac}} / 16\pi z_0 n_2$ . Taking  $n_0 = 1.45$ ,  $n_2 = 1.1 \times 10^{-13}$  cm<sup>2</sup>/statvolt<sup>2</sup> (Ref. 12) and  $z_0$  as calculated above, we obtain  $I_0 = 1.0 \times 10^6$  W/cm<sup>2</sup>. For our fiber<sup>17</sup> (core diameter 9.3  $\mu$ m), the effective core area,<sup>12, 18</sup>  $A_{\text{eff}} \cong 1.5 A_{\text{geom}}$ , or  $1.0 \times 10^{-6}$  cm<sup>2</sup>; thus  $(P_0)_{\text{theor}} \cong 1.0$  W. The average of  $P/N^2$  for the first three solitons yields  $(P_0)_{\text{expt}} \cong 1.24$  W. In view of the many uncertainties, the agreement here is quite good.

There is also a certain rough quantitative agreement in the time domain. The degree ( $\cong 3.5$  times) of pulse narrowing seen at  $P=5$  W is not quite the optimum predicted ( $\cong 5$  times) but the narrowing is reduced by deviation of the fiber length from  $z_0/2$ . The splitting (6.5 ps) measured at 11.4 W is  $\cong 1.5$  times greater than that predicted, but here asymmetry of the input pulse may have strong effects. A substantial asymmetry of the laser pulse is indeed indicated by the value, cited earlier, for the product  $\Delta t \Delta f$ , by the nearly Lorentzian shape of the frequency spectrum, and by the shape of the autocorrelation trace.

In conclusion, we have observed substantial compression and well-resolved splitting of picosecond pulses in the negative-dispersion region of a single-mode optical fiber. This behavior is in close agreement with prediction based on the nonlinear Schrödinger equation [Eq. (2)]. Although our input conditions can only approximate "exact" solitons, we have clearly observed their characteristic properties at the appropriate power levels.

We would like to thank A. Hasegawa for an illuminating discussion, W. J. Tomlinson for generating the computer solutions of Fig. 3, J. Simpson for the fiber, and H. Presby for information on its parameters. Also, special thanks to K. Iga for coating some mirrors for us and to A. M. Del Gaudio for considerable laboratory assistance.

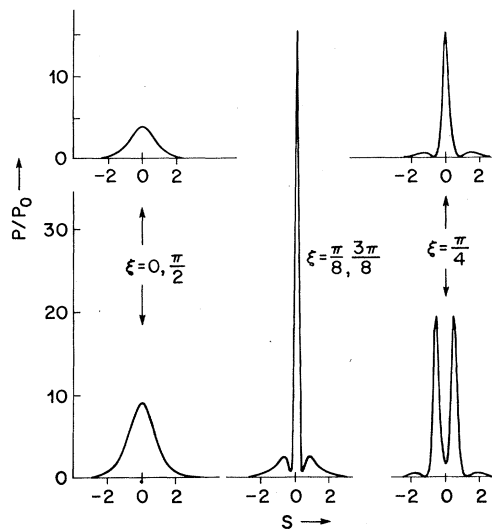


FIG. 3. Computer generated solutions to Eq. (2); above, the  $N=2$  soliton; below,  $N=3$  soliton. These solutions agree well with those indicated in Ref. 5. See text.

- <sup>1</sup>A. Hasegawa and F. Tappert, *Appl. Phys. Lett.* **23**, 142 (1973).
- <sup>2</sup>F. Tappert and A. Hasegawa, unpublished.
- <sup>3</sup>V. E. Zakharov and A. B. Shabat, *Zh. Eksp. Teor. Fiz.* **34**, 61 (1971) [*Sov. Phys. JETP* **34**, 62 (1972)].
- <sup>4</sup>V. E. Zakharov and A. B. Shabat, *Zh. Eksp. Teor. Fiz.* **64**, 1627 (1973) [*Sov. Phys. JETP* **37**, 823 (1973)].
- <sup>5</sup>J. Satsuma and N. Yajima, *Prog. Theor. Phys. Supp.* **55**, 284 (1974).
- <sup>6</sup>See, for example, *Solitons in Action*, edited by K. Lonngren and A. Scott (Academic, New York, 1978).
- <sup>7</sup>T. Miya, Y. Terunuma, T. Hosaka, and T. Miyashita, *Electron. Lett.* **15**, 106 (1979).
- <sup>8</sup>J. Simpson, *Am. Ceram. Soc. Bull.* **59**, 339 (1980).
- <sup>9</sup>L. F. Mollenauer and D. M. Bloom, *Opt. Lett.* **4**, 247 (1979).
- <sup>10</sup>The group-velocity dispersion  $D$ , often expressed in units of picoseconds per nanometer per kilometer, is given by  $D = (2\pi c/\lambda^2)\partial^2 k/\partial\omega^2 = v_g^{-2}\partial v_g/\partial\lambda$ . It is directly measurable in terms of the variation of pulse delay with wavelength in a fiber, and hence includes both material

and waveguide effects. Negative values of  $D$  have been termed "anomalous" in recent literature.

- <sup>11</sup>F. Shimizu, *Phys. Rev. Lett.* **19**, 1097 (1967); R. A. Fisher and W. K. Bischel, *J. Appl. Phys.* **46**, 4921 (1975).
- <sup>12</sup>R. H. Stolen and C. Lin, *Phys. Rev. A* **17**, 1448 (1978).
- <sup>13</sup>D. M. Bloom, L. F. Mollenauer, C. Lin, D. W. Taylor, and A. M. Del Gaudio, *Opt. Lett.* **4**, 297 (1979).
- <sup>14</sup>See Eq. (1) of Ref. 13.
- <sup>15</sup>See, for example, Chapt. 17 of G. B. Whitham, *Linear and Nonlinear Waves* (Wiley, New York, 1974).
- <sup>16</sup>Computer solution of Eq. (2) by W. J. Tomlinson, unpublished.
- <sup>17</sup>The fiber was of the step index type with a central index dip and had a Ge P-doped silica core and P silicate cladding; loss at  $1.55\ \mu\text{m}$  was  $\cong 1\ \text{dB/km}$ .
- <sup>18</sup>In connection with the matter of effective core area, an account of the effects of transverse variation can be found in B. Bendow, P. D. Gianino, N. Tzoar, and M. Jain, *J. Opt. Soc. Am.* **70**, 539 (1980).

## Frequency-Dependent Optical Dephasing in the Stoichiometric Material $\text{EuP}_5\text{O}_{14}$

R. M. Shelby and R. M. Macfarlane

*IBM Research Laboratory, San Jose, California 95193*

(Received 2 April 1980)

Optical coherent transients are reported here for the first time in a pure, optically concentrated material ( $\text{EuP}_5\text{O}_{14}$ ). Qualitatively new behavior is found in the form of a systematic variation of the homogeneous dephasing time  $T_2$  ( $\sim 20\ \mu\text{sec}$ ) across the inhomogeneously broadened line. This is interpreted as evidence for delocalization of the excitation. In contrast, the dilute impurity system  $\text{Eu}^{3+}:\text{YAlO}_3$  shows narrower lines and no frequency dependence of  $T_2$ .

PACS numbers: 42.65.Gv, 71.35.+z

Time-domain optical coherent transient phenomena<sup>1</sup> (e.g., photon echoes, optical free induction decay) provide the most generally useful and definitive way of measuring homogeneous dephasing times ( $T_2$ ). This is because measurements are made on the timescale of the dephasing itself, in contrast to most frequency domain techniques. So far, coherent transient measurements have been restricted to gas phase systems or isolated ionic or molecular impurities in solids.<sup>1</sup> This is in part due to a general belief that stoichiometric materials will exhibit extremely fast optical dephasing due to interactions between ions which lead to energy transfer, excitonic behavior, and rapid spectral diffusion. Dephasing measurements would, however, provide a fundamental means of characterizing the dynamics of these processes.

We report here the first measurement of coherent transients in a stoichiometric material, namely europium pentaphosphate ( $\text{EuP}_5\text{O}_{14}$ ). It is well known that rare-earth pentaphosphates exhibit high-yield intrinsic fluorescence and minimal trapping of the excitation, making them attractive materials for miniature solid-state lasers.<sup>2</sup> These properties imply that they have very narrow exciton bands and weakly delocalized excited states. Using the recently developed delayed-heterodyne photon-echo technique,<sup>3</sup> we find surprisingly long dephasing times of  $\sim 20\ \mu\text{sec}$ , which supports this picture. In addition, we find interesting and novel behavior in that the dephasing time varies in a systematic way as a function of position in the inhomogeneous line, indicating a corresponding variation in the nature of the excited state. This behavior is interpreted in